Integrated Multi-Omics Analysis of Mechanisms Underlying Yeast Ethanol Tolerance

Nikolina Šoštarić, Ahmed Arslan, Bernardo Carvalho, Marcin Plech, Karin Voordeckers,
Kevin J. Verstrepen, and Vera van Noort*

Cite This: *J. Proteome Res.* 2021, 20, 3840−3852

Read Online

ACCESS | Metrics & More | Article Recommendations | Supporting Information

ABSTRACT: For yeast cells, tolerance to high levels of ethanol is vital both in their natural environment and in industrially relevant conditions. We recently genotyped experimentally evolved yeast strains adapted to high levels of ethanol and identified mutations linked to ethanol tolerance. In this study, by integrating genomic sequencing data with quantitative proteomics profiles from six evolved strains (data set identifier PXD006631) and construction of protein interaction networks, we elucidate exactly how the genotype and phenotype are related at the molecular level. Our multi-omics approach points to the rewiring of numerous metabolic pathways affected by genomic and proteomic level changes, from energy-producing and lipid pathways to differential regulation of transposons and proteins involved in cell cycle progression. One of the key differences is found in the energy-producing metabolism, where the ancestral yeast strain responds to ethanol by switching to respiration and employing the mitochondrial electron transport chain. In contrast, the ethanol-adapted strains appear to have returned back to energy production mainly via glycolysis and ethanol fermentation, as supported by genomic and proteomic level changes. This work is relevant for synthetic biology where systems need to function under stressful conditions, as well as for industry and in cancer biology, where it is important to understand how the genotype relates to the phenotype.

KEYWORDS: genomics, quantitative proteomics, interactomics, ethanol tolerance, phenotype, yeast, signaling
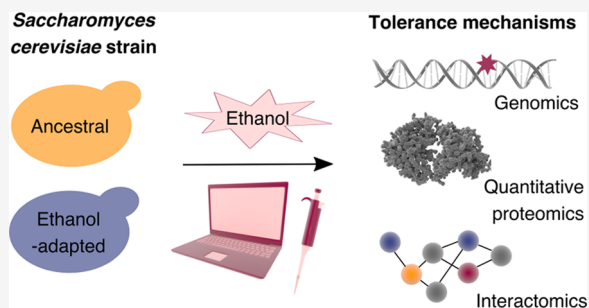
INTRODUCTION

Normal metabolic functioning of a yeast cell produces one of its most important stress-causing agents, ethanol. In high glucose and aerobic conditions, *Saccharomyces cerevisiae* uses glycolysis as its main source of adenosine triphosphate (ATP) and produces ethanol via aerobic fermentation, whereas respiration is repressed (known as the Crabtree effect), likely bringing yeast competitive advantages.[1,2] However, the increasing ethanol levels result in stress to yeast cells, ultimately leading to growth arrest and cell death. Cells have therefore developed a number of strategies to overcome the exposure to high levels of stress, typically by inducing cellular changes through regulatory networks.[2−5] Studies on the survival and adaptation mechanisms under ethanol assaults provide an ideal opportunity to identify and understand the regulatory events underlying this complex phenotype. It is well established that prolonged stress causes the accumulation of genomic mutations, which can in turn lead to adaptation.[6] Besides the acquisition of mutations, the consequences of ethanol stress range from slow growth, altered metabolic fluxes and biosynthetic activities, production of heat-shock proteins, larger cell size, and changes in protein abundances to cell death, reviewed elsewhere.[7] In a previous study, we discovered novel genetic mutations in budding yeast that were the result of exposure to increasing levels of ethanol over 200 generations.[8] The genetic variations that occurred during the course of these long-term evolutionary experiments are implicated in a diverse set of metabolic pathways.

Although many studies have focused on identification of specific mutations that increase ethanol tolerance, mechanistic insight into the long-term adaptation to high ethanol levels is still lacking. The details on how individual mutations contribute to cellular adaptation, the role of differentially regulated proteins in response to stress conditions, and how networks are rewired are unknown. This may partly be due to most studies using only a single type of omics data, while a multi-omics approach is required to identify precise regulatory events taking place during adaptation to ethanol stress.

In this work, we therefore aimed to elucidate the route from genomic and proteomic changes to the ethanol-tolerant phenotype in yeast. To this end, we developed an integrated
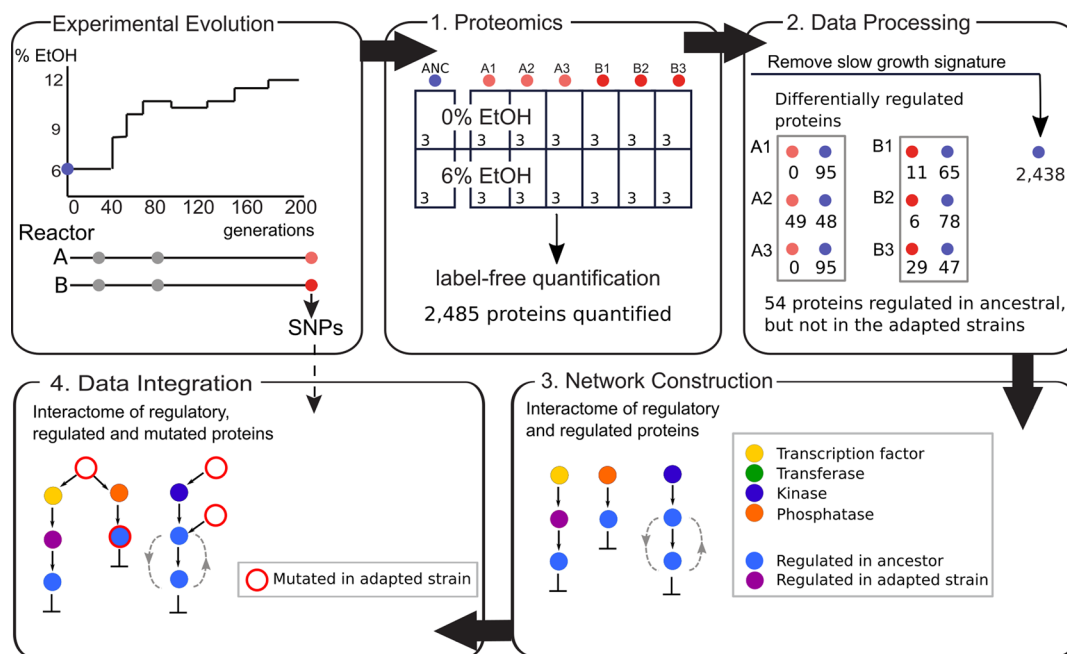
Figure 1. Overview of the workflow combining experimental and computational methods to unravel mechanisms underlying yeast ethanol tolerance. In our previous work (Voordeckers et al.[8]), ancestral yeast strain (ANC; shown in blue) was exposed to increasing ethanol concentration through 200 generations in two separate reactors (A and B); at the end point of the experimental evolution, three clones from each reactor (A1−A3 and B1−B3; shown in red) were sequenced. In this work, quantitative proteomics was performed using 3 technical replicates of each of these 6 ethanol-adapted clones, as well as the ancestral one, grown in either 0 or 6% ethanol (panel 1). After removing the slow growth signature proteins, differentially regulated proteins were identified in the data (panel 2) and used for the construction of protein−protein interaction networks (panel 3), in which the genomics data from our previous work has also been integrated (panel 4).

computational and experimental strategy (Figure 1) to understand the underlying ethanol tolerance mechanisms at the molecular level. More specifically, we performed label-free protein quantification on long-term stress-adapted yeast strains under two different conditions (0 and 6% ethanol). We then compared the protein abundance changes in response to ethanol in adapted strains with the ancestral strain and related the genomic mutations to the regulatory circuits in the context of ethanol stress. With our multi-omics strategy, we predict the contribution of specific proteins and mutations to potential cellular adaptation mechanisms and protein regulation patterns under ethanol stress.

EXPERIMENTAL PROCEDURES

Experimental Setup and Cell Growth

Evolved isolates were previously described[8] and all originated from a diploid, prototrophic *S. cerevisiae* S288c strain, which was grown in two separate reactors (A and B) through 200 generations of experimental evolution under increasing ethanol concentration (from 6 to 12% EtOH). For all culturing steps, filter-sterilized YPD (yeast extract, peptone, 4% dextrose) media was used. Filter sterilization was done using the Corning bottle-top vacuum filter system with a polyethersulfone membrane of 0.22 μm pore size. Three biological replicates of each strain (A1, A2, A3; B1, B2, B3) were grown in YPD (4% glucose) to early exponential phase ($OD_{600 \, nm} \sim 0.4$). Cultures were divided into two, spun down, washed once with YP, and one pellet was resuspended in YPD (4% glucose) while the other pellet was resuspended in YPD (4% glucose) supplemented with 6% EtOH (v/v). Cells were grown for two generations before sampling for global proteome profiling. Pellets were washed twice with phosphate-buffered saline

(PBS) to wash away any growth medium and subsequently frozen at −80 °C until further processing. A total of 42 samples were prepared for liquid chromatography−mass spectrometry (LC−MS)/MS analyses, belonging to biological triplicates of 7 strains (ancestral and 6 ethanol-adapted strains A1−B3) grown in 0 and 6% EtOH (v/v).

Mass Spectrometry and Protein Quantification

Sample Preparation and LC−MS/MS Analysis. The washed cell pellets were dissolved in 2 mL of lysis buffer (50 mM Hepes, 8 M urea) of which 500 μL was used to continue the protocol. Lysis was performed using FastPrep Lysis Matrix C beads. Tubes were vortexed 7 times for 10 s using a FastPrep machine at 4 °C. After that, the samples were sonicated to ensure complete lysis of the cells. Sonication was done with 5 pulses of 10 s at an amplitude of 20% using a VCX130 with a 3 mm probe (Sonics & Materials), whereas the complete lysis was observed under a microscope. After centrifugation to remove insoluble components, the supernatant containing around 500 μg of protein sample was used to continue with the protocol. Proteins were reduced (5 mM DTT, incubation for 30 min at 55 °C), alkylated (100 mM iodoacetamide for 15 min at room temperature in the dark), and digested by endo-LysC (2 μg LysC (Wako) (1/250, w/w) for 4 h at 37 °C), followed by overnight digestion with 5 μg of trypsin at 37 °C. The resulting peptide mixtures were desalted using C18 spin columns to remove excess reagents and urea. After elution from the C18 columns, aliquots containing 50 μg of peptides were dried completely by vacuum drying and stored at −20 °C. For LC−MS/MS analysis, samples were redissolved in batches of five before injection in 50 μL of 0.1% formic acid in water/acetonitrile (98:2, v/v) of which 2 μL was injected for LC−MS/MS analysis on an Ultimate 3000 RSLC nano LC

(Thermo Fisher Scientific, Bremen, Germany) in-line connected to a Q Exactive HF mass spectrometer (Thermo Fisher Scientific). The peptides were first loaded on a trapping column (made in-house, 100 μm internal diameter (ID) × 20 mm, 5 μm beads C18 Reprosil-HD, Dr. Maisch, Ammerbuch-Entringen, Germany). After flushing the trapping column, peptides were loaded in solvent A (0.1% formic acid in water) on a reverse-phase column (made in-house, 75 μm ID × 400 mm, 3 μm beads C18 Reprosil-Pur, Dr. Maisch) and eluted by an increase in solvent B (0.1% formic acid in acetonitrile) in linear gradients from 2 to 30% in 100 min and then from 30 to 56% in 40 min, followed by a washing step with 99% solvent B, all at a constant flow rate of 250 nL/min. The mass spectrometer was operated in data-dependent, positive ionization mode, automatically switching between MS and MS/MS acquisition for the 16 most abundant peaks in a given MS spectrum. The source voltage was set at 3.4 kV and the capillary temperature at 275 °C. One MS1 scan (m/z 375−1500, AGC target 3×10^6 ions, maximum ion injection time 60 ms), acquired at a resolution of 60 000 (at 200 m/z), was followed by up to 16 tandem MS scans (resolution 15 000 at 200 m/z) of the most intense ions fulfilling predefined selection criteria (AGC target 1×10^5 ions, maximum ion injection time 80 ms, isolation window 1.5 Da, fixed first mass 145 m/z, spectrum data type: centroid, minimum AGC target 1XE3, intensity threshold 1.3XE4, exclusion of unassigned, singly charged precursors, peptide match preferred, exclude isotopes on, dynamic exclusion time 12 s). The HCD collision energy was set to 32% normalized collision energy and the polydimethylcyclosiloxane background ion at 445.12003 Da was used for internal calibration (lock mass).

Protein Identification and Quantification. MS data analysis was performed with MaxQuant (version 1.5.3.30)[9] using the Andromeda search engine with default search settings including a false discovery rate (FDR) set at 1% on both the peptide and protein levels. Spectra were searched against a fasta file of UniProt[10] *S. cerevisiae* reference proteome combined with the amino acid sequences of mutated ORFs containing nonsynonymous single nucleotide polymorphisms (SNPs). The mass tolerance for precursor and fragment ions was set to 4.5 and 20 ppm, respectively, during the main search. Enzyme specificity was set as C-terminal to arginine and lysine, also allowing cleavage at proline bonds with a maximum of two missed cleavages. Variable modifications were set to oxidation of methionine residues and acetylation of protein N-termini and phosphorylation of serine, threonine, and tyrosine residues. Only proteins with at least one unique or razor peptide were retained leading to the identification of 3312 proteins. The proteins were quantified by the MaxLFQ algorithm, which is integrated in MaxQuant software. A minimum ratio count of two unique or razor peptides was required for quantification. Further data analysis was performed with Perseus software (version 1.5.2.6)[11] after loading the protein groups file from MaxQuant. The contaminants, proteins only identified by site, and reverse database hits were removed, and replicate samples were grouped. Proteins with less than three valid values in at least one group were removed and missing values were imputed from a normal distribution around the detection limit. This resulted in a list of 2485 quantified proteins.

Data Availability. The mass spectrometry proteomics data have been deposited to the ProteomeXchange Consortium via the PRIDE partner repository[12] and made public under the data set identifier PXD006631. The corresponding PRIDE project also contains detailed descriptions of sample preparation and MS data analysis.

Data Filtering

The compiled label-free protein quantification LC−MS/MS data consist of a repertoire of 2485 proteins. The regulated proteins may not reflect the direct consequences of ethanol stress but rather a general profile of slow growth, as suggested by O'Duibhir et al.[13] Among regulated proteins by ethanol, present in ethanol-adapted and nonadapted ancestor strains, a large number of proteins are up- or downregulated in the slow growth profile. These were filtered out and removed from our proteomics profiles for all further analysis, as suggested[13] (proteins with ‖log2 fold change|> 2 in O'Duibhir et al. (Figure 1)). This resulted in a reduced data set of 2438 proteins. We identified a set of proteins that are differentially regulated in 0 vs 6% of ethanol in both adapted and ancestral strains, as well as sets of proteins that are regulated in only one of those (either adapted strains or ancestral strain). Additionally, we put together six individual sets of proteins, one for each ethanol-adapted strain (A1−B3), that are either regulated in 0 vs 6% ethanol in the adapted strain but not in the ancestral strain or vice versa. Gene Ontology enrichments among regulated proteins were calculated using BiNGO in Cytoscape (version 3.4.0).[14] As background, all proteins identified by proteomics were used, i.e., 2438 proteins. The *p*-values were taken after FDR correction.

Protein Mutation and Copy Number Variation (CNVs) Data

The six ethanol-adapted clones were selected from two evolving populations, A and B, respectively[8] (Figure 1, step 1; see the section Experimental Setup and Cell Growth). The adapted populations contain single nucleotide polymorphisms (SNPs, detected in both A and B), as well as copy number variants (CNVs, detected only in A). The overlap between the mutated proteins between both samples was significant, but not complete. These mutations were integrated with protein abundance profiles in protein interaction networks to understand a possible role of mutations in protein regulation. The impact of SNPs on protein functional regions was determined using a Python script. NetPhosYeast 1.0 server[15] was used to check for the introduction of phosphorylation sites due to SNPs, GPS 5.0[16] to predict the kinase responsible for modification, and mutfunc[17] to predict functional consequences of introduced mutations. Where left noncited, information about protein function was retrieved from UniProt[10] or the *Saccharomyces* genome database.[18]

Protein Network (Re)construction and Data Integration

All yeast *S. cerevisiae* interactions were downloaded from the STRING database[19] to reconstruct an interaction network for proteins of interest. Only high-confidence yeast protein−protein interactions (combined_score > 0.7) were used in the workflow. The annotation of yeast regulatory proteins (transcription factors, kinases, phosphatases, and transferases) was retrieved from UniProt.[10] For the network construction, we started from all yeast regulatory proteins as "seed" and identified their direct interactors. For each of the 6 differentially regulated protein sets separately, the interactor of a regulatory protein was kept in the network if it is either (i) present in the differentially regulated protein list or (ii) is a protein with an SNP. This procedure was iterated to find interactors of interactors that are differentially regulated or
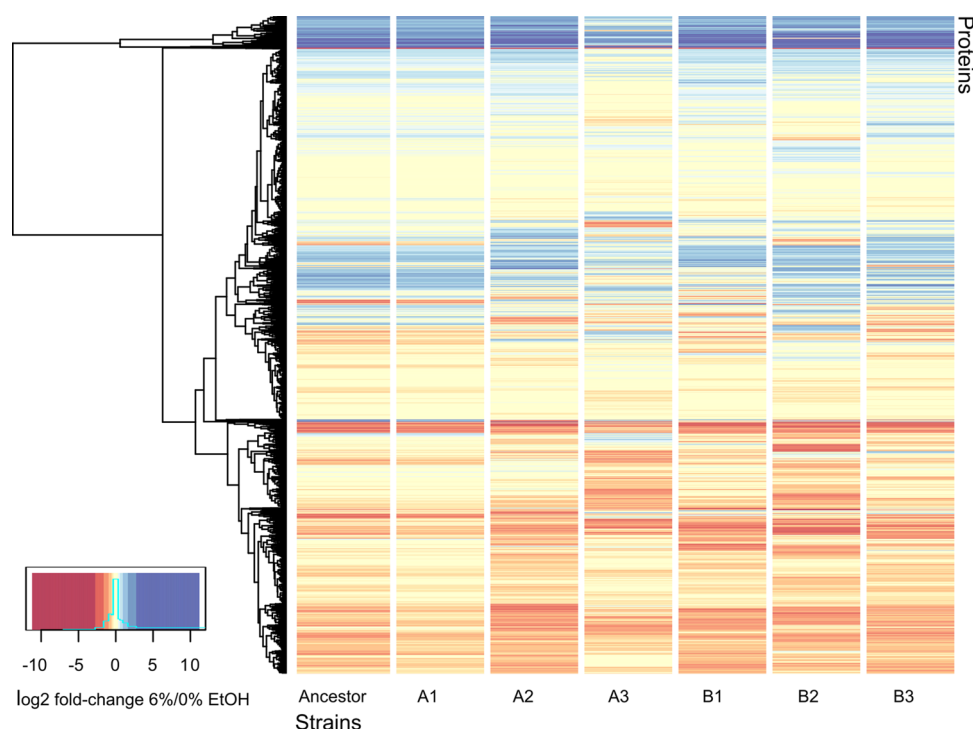
Figure 2. Heat map of log2 fold changes of protein abundance in six yeast strains adapted to high levels of ethanol and ancestral strain in 0 versus 6% ethanol.

have SNPs, until no new proteins were found for 6 sets (Figure 1, step 3). Finally, within each network, the edges were added between regulatory proteins, which are reported to interact (given that the combined_score is above 0.7). After the construction of 6 individual networks, one for differentially regulated, mutated, and regulatory proteins in each of the ethanol-adapted strains, individual interactions present in all 6 networks were collected to build a common network, to outline the omnipresent interactions.

■ RESULTS AND DISCUSSION

Quantitative proteomics and network analysis, combined with the previously identified genomic changes in ethanol-adapted yeast strains,[8] allowed us to reconstruct the route from these molecular level changes to the ethanol-tolerant phenotype. We start by taking a closer look into changes in protein abundance levels, which are specific to either ancestral or adapted strains, followed by metabolic implications of the observed genomic changes. Finally, we combine the two using protein interaction network analysis.

Ancestral and Adapted Strains Display Different Changes in Their Proteomes in Response to Ethanol Stress

In this study, we analyzed the proteomic response to 6% ethanol of wild-type yeast strain (ancestral) and 6 ethanol-adapted strains (experimentally evolved in increasing ethanol concentrations over 200 generations, termed A1−3 and B1−3) to obtain insight into the molecular mechanism of ethanol tolerance (Figure 1). Label-free quantitative proteomics was used to quantify a total of 2485 yeast proteins (Supporting Information Table S1, ProteomeXchange PXD006631). The proteins known to be regulated under conditions that induce slow growth were excluded from the data set to find the response that is specific for ethanol exposure.[13] This resulted in the reduced data set of 2438 quantified proteins (details in the section Experimental Procedures), which were used for all presented analyses.

The protein abundance levels between the ancestral and the adapted strains were not significantly different ($p < 0.01$) at 0% ethanol, suggesting it is the response to ethanol that is different in the ethanol-adapted strains. Overall, the proteomic response to ethanol is similar between the ancestor and ethanol-adapted strains (Figure 2). At the level of individual strains, no proteins were found to be significantly differentially regulated between 0 and 6% ethanol in 2 out of 6 adapted strains (A1 and A3, respectively; Supporting Information Tables S1 and S2), even though large log2 fold changes were observed (Figure 2). This is due to higher variance in protein expression, which deemed even the large log2 fold changes statistically nonsignificant in strains A1 and A3 (Supporting Information Table S1). These two those strains were consequently excluded from the remaining analyses in this section.

Adapted Strain-Specific Response to Ethanol Stress. We identified 3 proteins (Supporting Information Table S2) whose levels are significantly affected by ethanol in at least 3 out of 6 adapted strains, but not in the ancestral strain: Inh1, Lia1, and Suc2. Their regulation represents the long-term adaptation to stress acquired after prolonged exposure to increasing ethanol concentration.

Inh1 is the mitochondrial ATPase inhibitor that forms a one-to-one complex with this energy-producing machinery. Although Inh1 upregulation observed in this work might appear counterintuitive, given that energy metabolism is typically upregulated during stress,[20] our findings described in the following sections (proteome level changes and SNPs in Hem13 and Ppa2) support the model in which ethanol-adapted strains primarily use aerobic fermentation, while the ancestral switches to respiration. Inh1 upregulation is one of the changes working toward that end.

Lia1 is responsible for post-translational modification of lysine into hypusine. This unique modification is found in only one protein, eIF-5A factor, for whose biological activity it is essential. eIF-5A is involved in translation elongation[21] and is implicated in the cell cycle arrest—its depletion appears to halt the cell cycle progression by arresting cells in G1 phase,[22] presumably because eIF-5A is involved in the translation of proteins required for transition to S phase.[23] Lia1 down-regulation, observed in our proteomics data, could therefore have such an effect in our adapted strains.

Finally, Suc2, encoded by a high glucose-repressed gene, has a role in ethanol production through inulin degradation. A known consequence of the effect of ethanol on the cell membrane is the induction of a pseudo-starvation state, in which glucose from the medium cannot enter yeast cells.[24−26] Decrease in Suc2 protein level found here might therefore suggest that the adaptive changes in the evolved strains successfully worked toward (at least partially) suppressing pseudo-starvation.

Ancestor-Specific Response to Ethanol Stress. We identified 54 proteins that are significantly differentially regulated in the ancestral strain but not in at least 3 adapted strains (Supporting Information Table S2); 50% of these proteins were found to be upregulated, and the other 50% downregulated in response to ethanol. We found that some of the associated enriched biological processes are developmental maturation ($p = 5.70 \times 10^{-5}$) and transposition ($p = 1.01 \times 10^{-3}$). It has previously been suggested that increased gene expression of transposons may not be of adaptive significance but rather represent an opportunistic replication in weakened yeast cells.[27] Our data show that the ability to suppress the increase in transposon Ty1 and Ty2 protein levels is achieved exclusively in the ethanol-adapted strains. Interestingly, the upregulation of transposons in the ancestral strain is accompanied by downregulation of Ty1 transposition repress-or Rtt102. In addition to these changes, our proteomics findings demonstrate that the ancestral strain exposed to ethanol undergoes numerous protein level adjustments to slow down its growth, with the aim of reducing damage to cellular components and energy consumption for their repair. This is in agreement with previous reports of the correlation between slower cell growth and stress survival.[28] Herein, we identify differential regulation of proteins involved in ribosomal biogenesis, mitochondrial electron transport chain (mETC), transcription, nucleotide and amino acid metabolism, among others.

Ribosomal Biogenesis. We found 6 proteins involved in ribosomal biogenesis to be downregulated in ethanol stress. These proteins play roles in the maturation of the pre-60S ribosomal particle (Alb1),[29] biogenesis of 60S ribosomal subunit (Rsa3),[30] pre-mRNA splicing and pre-rRNA process-ing (Snu13), 20S pre-rRNA processing (Tsr2),[31] rRNA processing by associating with 90S pre-rRNA (Utp30),[32,33] and chaperoning Rsp3 ribosomal protein (Yar1).[34] The phenotypic consequences of their deletions differ from one protein to another; for example, Alb1 deletion does not seem to cause rRNA maturation impairment,[29] while Yar1 deletion reportedly causes 20S pre-rRNA accumulation and 40S export deficit.[34] Taken together, differential regulation of these proteins clearly works toward decreasing the number of available ribosomes and therefore silencing translation.

Transcription. Ncb2, Fip1, and Rpa14 were all found to be downregulated. Ncb2 is an essential component of the NC2 complex, which can both repress basal and stimulate activated transcription.[35] Yeast with reduced Ncb2 function was experimentally shown to exhibit slower growth,[36] so its downregulation observed here likely works toward the same end by impacting the transcript levels of protein-coding genes, possibly reducing their amount. On the other hand, Fip1 has a role in 3′ end mRNA processing, which is important in eukaryotes for transcript stability, export from the nucleus, and initiation of translation.[37−39] The main role of Fip1 is the inhibition of polyA synthesis enzyme Pap1; their interaction is essential for viability and was suggested as a mechanism for avoiding poly-adenylation of nontarget RNAs.[40] Taken together, it could be assumed that the reduced level of transcripts (due to Ncb2 regulation) in turn requires less regulation of Pap1 by Fip1. Finally, the observed down-regulation of RNA polymerase I component Rpa14 suggests that the ancestral strain also decreases production or rRNAs in response to ethanol.

Nucleotide Metabolism. Proteins involved in several pathways are differentially regulated in the ancestral strain: AMP production via salvage pathway (Apt1), purine nucleotide production via salvage pathway (Hpt1), de novo guanine nucleotide synthesis (Imd2), UMP biosynthesis via de novo pathway (Ura4), and CTP biosynthesis (Ura8). Down-regulation of all of these proteins, except Ura8, is also accompanied by downregulation of purine-cytosine permease Fcy2 level. As maintaining nucleotides pool level represents a necessary requirement for the growing cells, these down-regulations likely slow down the cell growth. In addition, limiting available nucleotides may also be an attempt toward antagonizing transposon upregulation.

Upregulated Ura8 plays a role in another part of metabolism important under ethanol stress, phospholipid synthesis,[41] as its reaction product (CTP) serves as a precursor of all membrane phospholipids synthesized via CDP-diacylglycerol and Ken-nedy pathways. Even though in normal conditions the majority of CTP is produced by the more abundant Ura7 enzyme, regulation of nondominant Ura8 observed in this work in ethanol stress probably occurs because of its different kinetic properties, as Ura8 is the preferred one in low ATP conditions.[41] This would be consistent with an increased energy demand for damage repair and maintenance of reactive oxygen species (ROS) levels (discussed below) in the ancestral strain.

Yet another strategy of slowing down the growth of the ancestral strain might be cell cycle delay through Ctf8 regulation. Its gene deletion was demonstrated to cause defects in sister chromatid cohesion, as well as G2/M cell cycle delay that requires Mad2-dependent mitotic spindle check-point.[42] A strong downregulation of Ctf8 level observed here in the ancestral strain might have a similar effect.

Amino Acid Metabolism. We observed differential regu-lation of proteins involved in lysine biosynthesis (Aco2 downregulation), methionine biosynthesis via salvage pathway (Adi1 downregulation, Aro9 upregulation), and leucine biosynthesis (Leu2 upregulation). Additionally, amino acid permease Agp1 was found to be downregulated. The role of amino acid biosynthesis pathways and accumulation of amino acids in ethanol tolerance is supported by previous studies, which show that increased levels of several amino acids (proline, valine, arginine, tryptophan) are linked to higher ethanol tolerance.[24,43,44]

Moreover, Snz1, involved in the synthesis of pyridoxal 5′-phosphate, was upregulated in our data. This cofactor is used by aminotransferases, transaminases, and glycogen metabolism enzymes, suggesting a possible way to increase the glucose level in pseudo-starvation. Further related to amino acid turnover, we observed upregulation of Add66, a protein required for optimal proteasome activity,[45] which could suggest increased protein degradation activity in ancestral strain. Although it has been reported that Add66 gene expression is induced by the unfolded protein response,[46] which includes halting of protein translation, degradation of misfolded proteins, and chaperone induction,[47] it is worth mentioning that we did not find the key factor for this response activation, Ire1, to be differentially regulated.

Our proteomics findings further show that the ancestral strain switches from ethanol fermentation to respiration, resulting in the production of 30 ATPs more per cycle.[2] This is in agreement with a recent study that combined metabolite profiling with carbon flux analysis using the *S. cerevisiae* metabolic model,[26] whose results suggested that ethanol stress exposure directs more carbon toward the tricarboxylic acid (TCA) cycle in the wild-type than in the ethanol-adapted yeast, thereby increasing respiration levels and decreasing ethanol production via fermentation. The authors further suggested that the switch from fermentative to respiratory growth might be the consequence of the increased energy demand for cell maintenance due to increased ROS production. However, it is also known that respiratory growth itself comes at a cost of increased ROS production on mitochondrial electron transport chain (mETC) components (mentioned below). Our data reveal the molecular actors behind the switch to respiration and further point to several proteome level changes in the ancestral strain that are aimed at controlling ROS levels.

Mitochondrial Electron Transport Chain. We observed Coa1, Coq8, Gut2, and Sdh7 to be upregulated in the ancestral strain, suggesting increased mETC usage. Coa1 is required for efficient assembly of mETC complex IV, while Coq8 is involved in the biosynthesis of coenzyme Q. Interestingly, we found Coq8 to be significantly downregulated in one of our adapted strains (B2). Although not directly involved in the synthesis and assembly of its components, Gut2 shuttle allows electrons from NADH produced in the cytoplasm to enter the mETC. Lastly, Sdh7 plays an essential role in the assembly of succinate dehydrogenase, which both participates in the TCA cycle and works as mETC complex II.

Autophagy. A recent study demonstrated that ethanol stress induces ROS (H_2O_2 and O_2^-) production, mainly on mETC components, so autophagy (Atg1 and Atg8) gene expressions were consequently induced to aid in eliminating ROS.[48] Our proteomics data are in line with these previous findings. Linked to the increased usage of the mETC described above, we observed a strong upregulation of the autophagy protein Atg8 in the ancestral strain. Interestingly, iron recycling through autophagy was previously found to be crucial for the transition from glycolytic to respiratory growth in yeast.[49]

Oxidative Stress Damage. Differentially regulated proteins involved in oxidative damage repair are Mxr1, Rpe1, Sam4, Srx1, Tma19, and Scp1. Downregulation of Mxr1, which has a role in repairing enzymes inactivated by oxidation, may be linked with Atg8 upregulation, as autophagy likely prevents protein damage by ROS removal. Along the same lines go downregulations of Rpe1 and Sam4. It was previously shown

that deletion of Tma19 enhances H_2O_2 stress resistance and prolongs the life span;[50] accordingly, we found this protein to be downregulated. Oppositely from that, oxidative stress resistance Srx1 was upregulated in our data. This protein, which is induced by increased H_2O_2 levels,[51] plays a unique role by repairing peroxiredoxin Tsa1, thereby contributing to protection from ROS. Finally, Scp1 binds to F-actin and induces the formation of tight bundles.[52] Its overexpression causes increased F-actin stability, which was linked to higher ROS levels and decreased cell viability.[53] On the contrary, Scp1 deletion was demonstrated as beneficial for cell longevity—actin may associate with mitochondrial channels, modulating their open/closed state, so slowing actin dynamics by Scp1 binding allows for a longer opening of the pores and subsequent ROS release to the cytoplasm. Downregulation of Scp1 observed in this work therefore likely represents yet another way to combat ROS production upon switch to respiration.

Finally, the remaining differentially regulated proteins with known cellular functions—Cit2 (upregulated), Sam50 (upregulated), and Zeo1 (downregulated)—are implicated in different parts of metabolism. A component of glyoxylate cycle in peroxisome, citrate synthase Cit2 was previously found to be regulated in low glucose conditions.[54] Cit2 uses acetyl-CoA originating from acetate or β-oxidation of fatty acids as a substrate, while the succinate produced in glyoxylate cycle can participate in the TCA cycle, with the final aim of glucose production via gluconeogenesis. Cit2 upregulation suggests that gluconeogenesis flux might be increased in the ancestral strain, as well as that the glucose level is rather low in this strain due to pseudo-starvation. Sam50 is involved in the assembly of the translocase of the outer membrane TOM, which is needed for the import of mitochondrial preproteins from the cytoplasm.[55] Lastly, differential regulation of Zeo1 has implications in the cell wall integrity, which is ensured through the Pkc1−Mpk1 pathway during cell wall stress.[56] Upstream from Pkc1 activation are Mid2 and Zeo1, with the first acting as positive and the latter as a negative regulator. Zeo1 downregulation may therefore underlie the activation of this pathway needed for cell wall integrity preservation under ethanol stress.

Common Response to Ethanol Stress. We identified 25 proteins that are significantly differentially regulated in both the ancestral and at least 3 ethanol-adapted strains, 22 of which are upregulated and 3 downregulated (Supporting Information Table S2). This group of proteins is linked to several biological processes, such as glycolysis ($p = 2.61 \times 10^{-3}$), gluconeogenesis ($p = 5.20 \times 10^{-3}$), and alcohol catabolic process ($p = 1.02 \times 10^{-2}$), confirming that yeast generally responds to ethanol stress by inducing changes in usage of energy-producing pathways.[20]

Significantly upregulated proteins involved in both glycolysis and gluconeogenesis (Supporting Information Figure S1) are Tdh1, Gpm2, and Eno1. Additionally, upregulation was observed for glycolysis-specific Pyk2 and gluconeogenesis-specific Pyc1, enzymes that catalyze the last and first (irreversible) reaction of the corresponding pathway. It was previously found that ethanol exposure causes a decrease in ethanol production and glucose uptake,[57] while others reported an increase in expression of genes related to glucose metabolism, including glucose transporters.[20] Gluconeogenesis could therefore also be important to compensate for the reduced glucose uptake, and produced glucose might be used

in the pentose phosphate pathway to produce NADPH required for biosyntheses. On the other hand, pyruvate produced by the glycolytic pathway is an important precursor for respiration. Understanding the differential regulation of other proteins, specific (described above) rather than common to ancestral and adapted strains, is therefore crucial to understand to which extent each of these pathways is used in each strain.

Further related to the glucose metabolism, we have identified differential regulation of hexose (glucose) transporters—low-affinity Hxt1 and high-affinity Hxt2 down-regulation, and high-affinity Hxt7 upregulation—which is in line with the gene expression changes observed by Chandler et al.[25] and aimed at increasing glucose uptake during the ethanol-induced pseudo-starvation. More specifically, we found no major differences in Hxt1 and Hxt2 level changes between the ancestral and adapted strains, while log2 fold change for Hxt7 was higher in ethanol-adapted strains (5.5−8.1 compared to 3.8 in the ancestral). This might suggest that the ethanol-adapted strains are more successful in antagonizing pseudo-starvation, aiding their return to fermentative growth. Moreover, we have observed increased levels of Nth1, which converts trehalose (made of two glucose units) to glucose. Trehalose accumulation was reported to be beneficial for ethanol tolerance[43,44,58,59] and the suggested mechanism is 2-fold: (i) trehalose acts as a chemical co-chaperone, preventing aggregation of misfolded proteins to the membrane, and (ii) it displaces water and ethanol from the membrane, thereby stabilizing it.[58] Nth1 upregulation found here, which would work toward an increase of the intracellular glucose level, might therefore represent yet another mechanism in which trehalose protects from ethanol stress.

We also found that stress response affected proteins linked to phosphate and NAD(P)H. More specifically, Pho5 upregulation was observed in all strains of this study. This secreted phosphatase has a major role in acquiring the extracellular phosphate and was previously reported as upregulated in phosphate-scarce conditions.[60] Furthermore, we have observed the upregulation of epimerase Nnr1 and dehydratase Nnr2, which work together to repair hydration-damaged NAD(P)H. These two enzymes may therefore play a role in energy metabolism through increasing the pool of the available NADH, as well as in reductive biosyntheses by increasing the amount of usable NADPH.

Mitochondrial outer membrane channel Por1 is yet another upregulated protein in ethanol stress, reported to have several roles. For example, its role in glucose level sensing occurs through positive control of Snf1 kinase[61]—in limited glucose conditions (such as pseudo-starvation, especially in the ancestral strain); Snf1 activation[62] triggers repression release of genes for gluconeogenesis, respiration, and uptake of alternative carbon sources.[4] It was also suggested that Por1 permeability depends on the rate of glycolysis, as cytosolic NADH causes Por1 closure and subsequent decrease in respiration. Por1 may therefore be involved in glucose-induced suppression of respiration in our adapted strains. Finally, deletion of Por1 was shown to cause a decrease in cardiolipin levels and loss of phosphatidylethanolamine synthesis,[63] suggesting a link between Por1 regulation and membrane remodeling.

Finally, we observed downregulation of purine salvage pathway protein Aah1 (similar changes were described above for the ancestral strain), as well as upregulation of Hsp31 and Prx1 involved in oxidative stress protection.

Connection of Copy Number Variants to Protein Abundance Changes

In our previous work, we have identified copy number variations (CNVs) in several genes of ethanol-tolerant strains A1, A2, and A3 after 200 generations of experimental evolution.[8] When combined with the quantitative proteomics data from the present study, the question arises whether the CNVs are accompanied by changes in protein abundance levels. Because there are many regulatory mechanisms for maintaining protein levels, it is not obvious that copy number gains or losses would affect protein abundances: transcription, mRNA stability, translation, and protein degradation together dictate the amount of the available protein.[64] Although we found no genes with CNVs among proteins differentially regulated in response to ethanol only in adapted strains, 7 genes with CNVs were identified among those differentially regulated only in the ancestral strain. For instance, Imd2 has both copy number loss and significant protein level down-regulation in response to ethanol in the ancestral strain. Different from this, amino acid permease Agp1 has copy number gain while being downregulated, confirming a lack of a clear link between the CNVs of protein-coding genes and changes in protein abundance under ethanol stress. This finding is in agreement with previous research.[65]

Nonsynonymous Protein Mutations in Stress Conditions

We have previously identified single nucleotide polymorphisms (SNPs) in 6 ethanol-adapted diploid yeast strains at the end point (200 generations) of two independent evolutionary experiments (Figure 1A,B).[8] Effects of these SNPs vary from the introduction of STOP codons and amino acid substitutions to synonymous changes (Supporting Information Table S3). Seven SNPs were identified in all 6 adapted strains: STOP codons introduction to Rap1, Dsk2, Asg1, and Faa4, resulting in truncated, likely nonfunctional proteins; and amino acid substitutions Mrpl37_Arg89Ser, Hem13_Ala234Pro, and Ppa2_Ala128Ser. The omnipresence of these SNPs indicates the potentially universal and crucial changes that allow yeast survival in highly stressful conditions (12% ethanol), given that they arose in all clones of two independently evolving populations.

Truncated Proteins. It was previously reported that ethanol stress causes telomere elongation in yeast, with Rap1 and Rif1 as crucial actors in this response.[66] More specifically, Rif1 and Rif2 are negative regulators of telomere length, which interact with the C-terminus of telomere-binding Rap1.[67] Rap1 downregulation (found in ethanol stress[66]), or mutations in Rap1 C-terminus, was therefore reported to cause telomere elongation, as well as heterogeneity in telomere lengths.[68,69] Although our adapted strains acquired a STOP codon-introducing SNP at position 605 in Rap1 (total protein length 827 amino acids), the ancestral strain exhibited a slight (though not statistically significant) downregulation of Rap1 protein level, confirming the importance of Rap1 silencing under ethanol stress.

Dsk2 is involved in the ubiquitin-proteasome proteolytic pathway through recruiting K48-ubiquitylated proteins for degradation[70] and was previously reported to become essential under salt stress.[71] Its deletion was found to have little effect on protein degradation as Dsk2 is partially functionally redundant with Rad23.[72] On the other hand, Dsk2 over-

Table 1. Experimentally Determined Phenotypes of Deletion Mutants, with Focus on the Effects on Respiratory Growth, Based on the Information from the *Saccharomyces* Genome Database (SGD)

strain	protein	functional role	ethanol effect	SGD phenotype: respiratory growth
adapted	Inh1	mitochondrial ATPase inhibitor	upregulated	NA
adapted (B2 clone)	Coq8	coenzyme Q biosynthesis	downregulated	null and point mutants are unable to respire and fail to accumulate ubiquinones
adapted	Hem13	heme biosynthesis	Ala234Pro	mutants fail to respire
adapted	Ppa2	mitochondrial inorganic phosphatase	Ala128Ser	respiratory growth absent in null mutants
ancestral	Coa1	mETC complex IV assembly	upregulated	null mutant shows greatly diminished respiratory metabolism and growth
ancestral	Coq8	coenzyme Q biosynthesis	upregulated	null and point mutants are unable to respire and fail to accumulate ubiquinones
ancestral	Gut2	NADH shuttling to mETC	upregulated	respiratory growth decreased in null mutants
ancestral	Sdh7	mETC complex II assembly	upregulated	respiratory growth decreased or absent in null mutants

expression appears to be toxic for cells, causing not only accumulation of ubiquitylated substrates but also cell cycle arrest. By ubiquitylating Dsk2 and proteasome subunit Rpn10, both of which are involved in degradation of cyclins,[70] Rad7 ultimately regulates spindle pole body proteins to fine-tune cell cycle checkpoint activation due to DNA damage. Rendering Dsk2 inactive by the introduction of a STOP codon, observed here in the ethanol-adapted strains, could therefore interfere with this checkpoint. Weakening cell cycle checkpoints might represent a more general strategy to continue the cell growth despite the existing stress-damaged DNA sites, instead of halting it for multiple repair and checkpoint cycles.

Numerous studies have established the link between ethanol stress resistance and changes in membrane composition, more specifically the level of fatty acid saturation of membrane lipids.[73] It is well described that ethanol stress increases fluidity and decreases the stability of the membrane, the effects caused by the replacement of water by ethanol in interactions with phospholipids in the bilayer.[58] A major membrane remodeling is a known adaptation strategy, allowing yeast cells to become less susceptible to ethanol.[43] Asg1 and Faa4, both affected by a STOP codon-introducing SNP, might be involved in these changes. Faa4 is directly implicated in lipid metabolism, more specifically esterification of free fatty acids (FFAs), originating from lipid degradation or exogenous pool, into metabolically active acyl-CoA. Faa1, Faa2, Faa3, and Fat1[74] (Supporting Information Figure S2) all catalyze the same reaction; however, Faa1, Faa4, Fat1 have dominant roles. Their functioning is so far mainly investigated in the context of lipid over-production.[75] In contrast to Faa4, Asg1 has an indirect role in the lipid metabolism, as it is required for activation of proteins involved in β-oxidation (Pox1, Pot1, Fox2), gluconeogenesis (Pck1), glyoxylate cycle (Icl1), triacylglycerol (TAG) breakdown (Tgl3), and peroxisomal transport (Pxa1).[76] Previous studies have reported accumulation of TAG and FFA upon *asg1* deletion[76] (Supporting Information Figure S2). Furthermore, as Asg1 appears to be required for full activation of gluconeogenesis enzyme Pck1 (Supporting Information Figure S1), Asg1 inactivation might favor glycolysis over gluconeogenesis.

Taken together, truncations of Asg1 and Faa4 in the adapted strains might serve as a way to redirect fatty acids into membrane lipid production instead of employing them as an energy source through β-oxidation. It could also be hypothesized that membrane restructuring makes exogenous FFA uptake more difficult, which would leave lipid synthesis in the cell as the main source of fatty acyl-CoA. Moreover, as reductive biosyntheses such as lipid production require

NADPH, it is likely that the pentose phosphate pathway also has an important role. Assuming that both NADPH and ATP are required, NADPH would be produced in the first phase of the pentose phosphate pathway, while the ribose 5-phosphate would be converted to fructose 6-phosphate to take part in the ATP-producing steps of glycolysis, further suggesting that glycolysis is favored over gluconeogenesis in ethanol-adapted strains.

Amino Acid Substitutions. Nonsynonymous amino acid substitutions identified in Mrpl7, Hem13, and Ppa2 are predicted by mutfunc[17] to have functional impacts as they affect conserved amino acids (Supporting Information Table S3). Mrpl37 works as a component of the mitochondrial ribosome[77] and its Arg89Ser substitution is predicted by NetPhosYeast[15] to introduce a phosphorylation site, with Ste7 as the predicted corresponding kinase. The mechanisms through which this phosphorylation site introduction aids in acquiring ethanol tolerance remain to be tackled. The remaining two proteins, Hem13 and Ppa2, are related to mETC, with Hem13 involved in the biosynthesis of heme, an essential part of the mETC complex IV, and mitochondrial inorganic phosphatase Ppa2 listed among the proteins essential for respiration. Interestingly, *ppa2* deletion was reported as beneficial for cell longevity, and the proposed deficiency in respiration was hypothesized to be compensated through the usage of the glycolytic pathway.[78] Differently from Mrpl37, no phosphorylation site introduction is predicted due to Ala128Ser in Ppa2, whereas Ala234Pro substitution in Hem13 is predicted to destabilize the protein ($\Delta\Delta G$ = 6.9 kcal/mol). Together, SNPs in Hem13 and Ppa2 likely represent permanent changes working toward disruption of mETC usage and restoring the fermentative growth upon achieving ethanol tolerance.

Fermentation vs Respiration: Phenotypes of Gene Deletion Strains

To validate our findings on different uses of glycolysis and mETC between ancestral and ethanol-adapted strains, we examined the experimentally determined phenotypes reported for deletion (null) mutants of the relevant genes using data from the *Saccharomyces* genome database[18] (Table 1). These experimental findings support the model in which SNPs and protein level changes in the ethanol-adapted yeast strains prevent respiration usage and favor aerobic fermentation. On the contrary, the ancestral strain switches from fermentative to respiratory growth, thereby increasing ATP production but also suffering increased ROS levels.
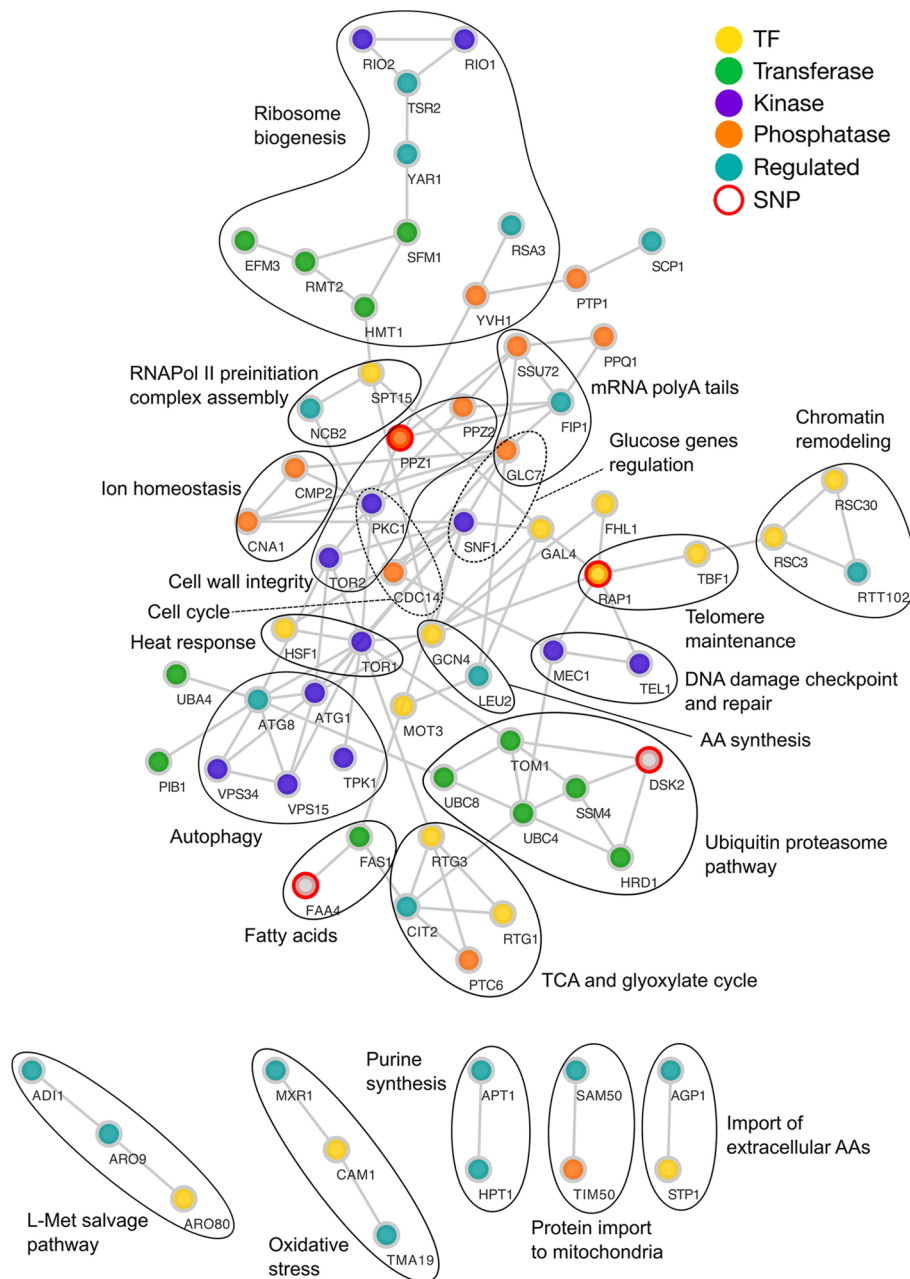
Figure 3. High-confidence protein–protein interaction network of differentially regulated, mutated, and regulatory proteins common to all 6 ethanol-adapted strains.

Common Interaction Network

To understand protein regulation in ethanol-adapted strains, we performed a protein–protein interaction network construction prioritizing potential yeast regulatory and mutated proteins (Figure 1, steps 3 and 4). Regulatory proteins were used as seed proteins, whose interactors were only kept in the network if they are differentially regulated in an adapted but not in the ancestral strain, or vice versa, or if they were identified as affected by SNPs in the given adapted strain. A total of six networks (one for each adapted strain; Supporting Information Figure S3) were constructed and subsequently compared to identify the common protein–protein interaction sub-network (Figure 3).

Proteins in our common network are involved in numerous cellular processes (Figure 3), such as ribosome biogenesis,

ubiquitin-proteasome pathway, chromatin remodeling, DNA repair, cell cycle, and autophagy. This is similar to the findings of a recent study focused on salt stress in *S. cerevisiae*, which also combined experimental (transcriptome, phosphoproteome) and protein interaction data.[3] Their results revealed significant connectivity between different pathways, suggesting signal integration, which happens either directly or through integration points. The latter may prevent signaling crosstalk, or coordinate magnitude or timing of the signaling, among other possible roles. More specifically, the salt stress study found Cdc14 to be such a signal integrator, bridging Hog and Ck2 signaling, as well as connecting to pathways such as Tor1, which is reportedly repressed by Cdc14.

In our network, several proteins appear to have central roles, such as Pkc1, Tor1, and Tor2, and previously mentioned glucose-sensing Snf1. In addition, Cdc14 is also present, the
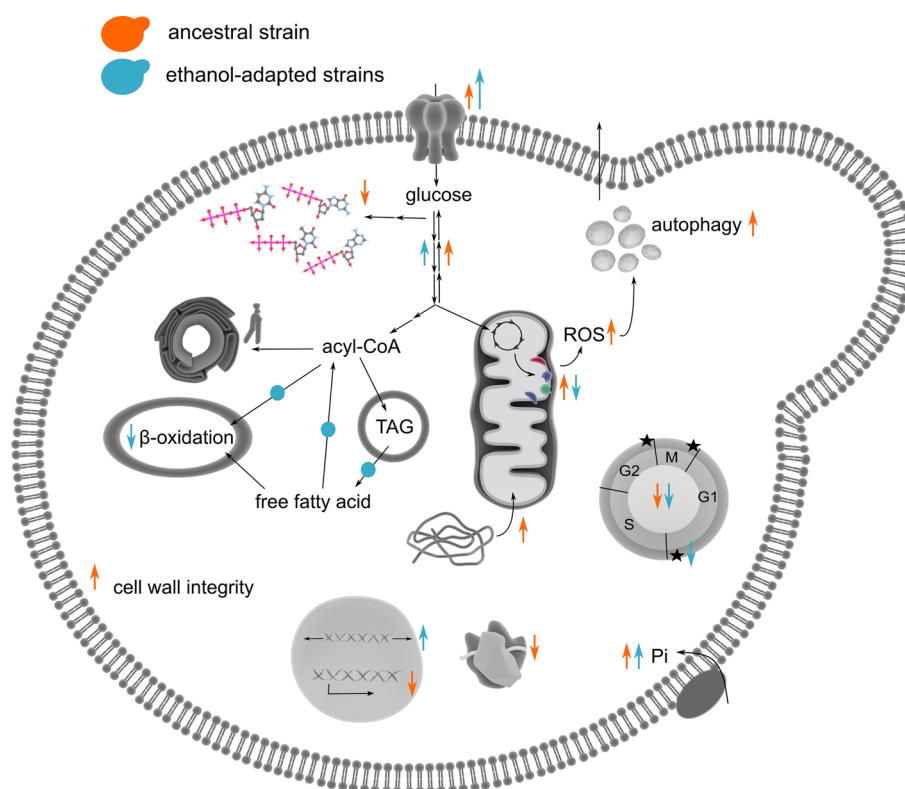
Figure 4. Yeast cell scheme summarizing the key findings. Upward arrows denote upregulation and downward arrows downregulation, while different colors stand for ancestral and ethanol-adapted strains.

same as in the salt stress. Pkc1 kinase is known to be involved in a number of processes: (i) cell growth and transition from G2 to M phase, (ii) cell wall integrity through its role in the Pkc1−Mpk1 cascade, (iii) cell cycle arrest in the face of DNA damage, as it activates DNA double-strand break repair sensors Mec1 and Tel1 (also present in the network), and (iv) autophagy, among others.[79] Tor kinases are central components of a major signaling network that controls cellular growth.[4] Yeast has two functionally distinct complexes: TORC1 (containing both Tor homologs), regulating temporal aspects of cell growth, and TORC2 (containing Tor2 but not Tor1), responsible for spatial aspects of cell growth. TORC1 is involved in triggering the corresponding cellular response based on nutrient availability and affects transcription, translation, and post-translational modifications, among others.[2,4] TORC1 inhibition leads to cell cycle arrest, protein synthesis downregulation, as well as upregulation of autophagy, and trehalose and stress response genes.[4] On the other hand, TORC2 is involved in the polarization of the actin cytoskeleton and is related to the cell wall integrity pathway.

■ CONCLUSIONS

To contribute toward the understanding of processes underlying ethanol stress response in *S. cerevisiae*, we performed an integrated analysis of genomics and proteomics data using ethanol-adapted yeast strains. Furthermore, we developed a protein interaction network reconstruction strategy from multiomics data: we combined genomic mutations with quantitative proteomics and yeast interactome to identify rewired regulatory networks in the adapted strains. In comparison to previous sub-network search strategies for yeast regulome,[3,80] our strategy does not rely on sub-network(s) identification and

identification of regulatory proteins therein. Instead, we constructed connected networks starting from yeast regulatory proteins to identify regulators that are directly connected to networks of differently regulated proteins.

Our approach allowed us to identify potential regulatory consequences of protein mutations and key regulated proteins (Figure 4). The ancestral strain appears to respond to ethanol stress by halting energy production mainly via ethanol fermentation, in which ethanol must be produced to regenerate NAD⁺. To satisfy the energy requirements of the cell under such conditions, ancestral yeast increases its usage of mETC and respiration (Coa1, Coq8, Gut2, Sdh7), which in turn increases the production of ROS. Consequently, autophagy is induced to remove these harmful molecular species (Atg8). The ethanol stress-induced pseudo-starvation is likely antagonized both through the increased gluconeogenesis flux and increased levels of high-affinity hexose transporters. Other metabolic changes in the ancestral yeast include repression of ribosome biogenesis, transcription, and nucleotide metabolism, which together slow down cell growth, thereby reducing the amount of damage that the cell has to repair in an energy-consuming fashion. In addition, protein degradation (Add66), phospholipid synthesis (Ura8), and cell wall integrity pathway (Zeo1) are stimulated, while the cell cycle may be delayed (Ctf8).

On the other hand, the ethanol-adapted strains appear to return to aerobic fermentation instead of respiration as the main source of ATP. This metabolic change is supported by both proteomics and genomics data presented in this work (Inh1, Ppa2, Hem13, Coq8). These strains also appear to be better adapted to deal with the pseudo-starvation state (Suc2, Hxt7), likely as a consequence of a (partially) remodeled cell

membrane and even higher protein levels of hexose transporters compared to the ancestral strain. Moreover, genetic mutations acquired by the adapted strains allow for beneficial telomere elongation (Rap1), rewire phospholipid metabolism (perhaps to use them for membrane remodeling rather than an energy source; Asg1 and Faa4), and potentially weaken cell cycle checkpoint activation (Dsk2). The latter might have a role in allowing the cells to grow, divide, and therefore adapt more easily, despite being exposed to highly stressful conditions. In addition, glycolysis flux appears to dominate gluconeogenesis. Finally, network reconstruction reveals a high level of interconnectedness of these relevant pathways on a protein interaction level. Taken together, our findings provide an insight into short- and long-term adaptation mechanisms and the key molecular actors that allow the yeast to survive under ethanol stress.

■ ASSOCIATED CONTENT

ⓈⒾ Supporting Information

The Supporting Information is available free of charge at https://pubs.acs.org/doi/10.1021/acs.jproteome.1c00139.

> Differentially regulated proteins in glycolysis and gluconeogenesis (Figure S1); metabolic pathways affected by SNPs in *faa4* and *asg1* genes (Figure S2); protein interaction network of regulatory, differentially regulated and mutated proteins in each of the 6 ethanol-adapted strains (Figure S3) (PDF)

> Overview of differentially regulated proteins (quantitative proteomics data) and copy number variants (Table S2) (XLSX)

> SNPs identified in ethanol-adapted strains and their predicted impact on protein function (Table S3) (XLSX)

> Quantitative proteomics data overview (full data set available at ProteomeXchange PXD006631) (Table S1) (XLSX)

■ AUTHOR INFORMATION

Corresponding Author

Vera van Noort − *Centre of Microbial and Plant Genetics, KU Leuven, B-3001 Leuven, Belgium; Institute of Biology Leiden, Faculty of Science, Leiden University, 2333 BE Leiden, The Netherlands*; Phone: +32 16 37 92 16; Email: vera.vannoort@kuleuven.be

Authors

Nikolina Šoštarić − *Centre of Microbial and Plant Genetics, KU Leuven, B-3001 Leuven, Belgium*

Ahmed Arslan − *Centre of Microbial and Plant Genetics, KU Leuven, B-3001 Leuven, Belgium;* Present Address: Stanford University School of Medicine, 300 Pasteur Drive, Stanford, California 94305, United States.

Bernardo Carvalho − *Centre of Microbial and Plant Genetics, KU Leuven, B-3001 Leuven, Belgium*

Marcin Plech − *Centre of Microbial and Plant Genetics, KU Leuven, B-3001 Leuven, Belgium; VIB-KU Leuven Center for Microbiology, Bioincubator, B-3001 Leuven, Belgium*

Karin Voordeckers − *Centre of Microbial and Plant Genetics, KU Leuven, B-3001 Leuven, Belgium; VIB-KU Leuven Center for Microbiology, Bioincubator, B-3001 Leuven, Belgium*

Kevin J. Verstrepen − *Centre of Microbial and Plant Genetics, KU Leuven, B-3001 Leuven, Belgium; VIB-KU Leuven Center for Microbiology, Bioincubator, B-3001 Leuven, Belgium*

Complete contact information is available at:
https://pubs.acs.org/10.1021/acs.jproteome.1c00139

Notes

The authors declare no competing financial interest.

■ ACKNOWLEDGMENTS

■ ABBREVIATION LIST

CNV, copy number variant; CoA, coenzyme A; FFA, free fatty acid; mETC, mitochondrial electron transport chain; NAD(P)H, nicotinamide adenine (di)nucleotide (phosphate); ROS, reactive oxygen species; SNP, single nucleotide polymorphism; TAG, triacylglycerol; TCA cycle, tricarboxylic acid cycle; TF, transcription factor

■ REFERENCES

(1) De Deken, R. H. The Crabtree Effect: A Regulatory System in Yeast. *J. Gen. Microbiol.* **1966**, *44*, 149−156.

(2) Broach, J. R. Nutritional Control of Growth and Development in Yeast. *Genetics* **2012**, *192*, 73−105.

(3) Chasman, D.; Ho, Y.-H.; Berry, D. B.; Nemec, C. M.; MacGilvray, M. E.; Hose, J.; Merrill, A. E.; Lee, M. V.; Will, J. L.; Coon, J. J.; Ansari, A. Z.; Craven, M.; Gasch, A. P. Pathway Connectivity and Signaling Coordination in the Yeast Stress-Activated Signaling Network. *Mol. Syst. Biol.* **2014**, *10*, No. 759.

(4) Smets, B.; Ghillebert, R.; De Snijder, P.; Binda, M.; Swinnen, E.; De Virgilio, C.; Winderickx, J. Life in the Midst of Scarcity: Adaptations to Nutrient Availability in *Saccharomyces cerevisiae*. *Curr. Genet.* **2010**, *56*, 1−32.

(5) Steensels, J.; Verstrepen, K. J. Taming Wild Yeast: Potential of Conventional and Nonconventional Yeasts in Industrial Fermentations. *Annu. Rev. Microbiol.* **2014**, *68*, 61−80.

(6) Galhardo, R. S.; Hastings, P. J.; Rosenberg, S. M. Mutation as a Stress Response and the Regulation of Evolvability. *Crit. Rev. Biochem. Mol. Biol.* **2007**, *42*, 399−435.

(7) Stanley, D.; Bandara, A.; Fraser, S.; Chambers, P. J.; Stanley, G. A. The Ethanol Stress Response and Ethanol Tolerance of *Saccharomyces cerevisiae*. *J. Appl. Microbiol.* **2010**, *109*, 13−24.

(8) Voordeckers, K.; Kominek, J.; Das, A.; Espinosa-Cantú, A.; De Maeyer, D.; Arslan, A.; Van Pee, M.; van der Zande, E.; Meert, W.; Yang, Y.; Zhu, B.; Marchal, K.; DeLuna, A.; Van Noort, V.; Jelier, R.; Verstrepen, K. J. Adaptation to High Ethanol Reveals Complex Evolutionary Pathways. *PLoS Genet.* **2015**, *11*, No. e1005635.

(9) Cox, J.; Mann, M. MaxQuant Enables High Peptide Identification Rates, Individualized p.p.b.-Range Mass Accuracies and Proteome-Wide Protein Quantification. *Nat. Biotechnol.* **2008**, *26*, 1367−1372.

(10) UniProt Consortium. UniProt: A Worldwide Hub of Protein Knowledge. *Nucleic Acids Res.* **2019**, *47*, D506−D515.

(11) Tyanova, S.; Temu, T.; Sinitcyn, P.; Carlson, A.; Hein, M. Y.; Geiger, T.; Mann, M.; Cox, J. The Perseus Computational Platform

for Comprehensive Analysis of (Prote)Omics Data. *Nat. Methods* **2016**, *13*, 731−740.

(12) Vizcaíno, J. A.; Côté, R. G.; Csordas, A.; Dianes, J. A.; Fabregat, A.; Foster, J. M.; Griss, J.; Alpi, E.; Birim, M.; Contell, J.; O'Kelly, G.; Schoenegger, A.; Ovelleiro, D.; Pérez-Riverol, Y.; Reisinger, F.; Ríos, D.; Wang, R.; Hermjakob, H. The Proteomics Identifications (PRIDE) Database and Associated Tools: Status in 2013. *Nucleic Acids Res.* **2012**, *41*, D1063−D1069.

(13) O'Duibhir, E.; Lijnzaad, P.; Benschop, J. J.; Lenstra, T. L.; Leenen, D.; Groot Koerkamp, M. J.; Margaritis, T.; Brok, M. O.; Kemmeren, P.; Holstege, F. C. Cell Cycle Population Effects in Perturbation Studies. *Mol. Syst. Biol.* **2014**, *10*, 732.

(14) Maere, S.; Heymans, K.; Kuiper, M. BiNGO: A Cytoscape Plugin to Assess Overrepresentation of Gene Ontology Categories in Biological Networks. *Bioinformatics* **2005**, *21*, 3448−3449.

(15) Ingrell, C. R.; Miller, M. L.; Jensen, O. N.; Blom, N. NetPhosYeast: Prediction of Protein Phosphorylation Sites in Yeast. *Bioinformatics* **2007**, *23*, 895−897.

(16) Xue, Y.; Ren, J.; Gao, X.; Jin, C.; Wen, L.; Yao, X. GPS 2.0, a Tool to Predict Kinase-Specific Phosphorylation Sites in Hierarchy. *Mol. Cell. Proteomics* **2008**, *7*, 1598−1608.

(17) Wagih, O.; Galardini, M.; Busby, B. P.; Memon, D.; Typas, A.; Beltrao, P. A Resource of Variant Effect Predictions of Single Nucleotide Variants in Model Organisms. *Mol. Syst. Biol.* **2018**, *14*, No. e8430.

(18) Cherry, J. M.; Hong, E. L.; Amundsen, C.; Balakrishnan, R.; Binkley, G.; Chan, E. T.; Christie, K. R.; Costanzo, M. C.; Dwight, S. S.; Engel, S. R.; Fisk, D. G.; Hirschman, J. E.; Hitz, B. C.; Karra, K.; Krieger, C. J.; Miyasato, S. R.; Nash, R. S.; Park, J.; Skrzypek, M. S.; Simison, M.; Weng, S.; Wong, E. D. Saccharomyces Genome Database: The Genomics Resource of Budding Yeast. *Nucleic Acids Res.* **2012**, *40*, D700−D705.

(19) Szklarczyk, D.; Gable, A. L.; Lyon, D.; Junge, A.; Wyder, S.; Huerta-Cepas, J.; Simonovic, M.; Doncheva, N. T.; Morris, J. H.; Bork, P.; Jensen, L. J.; Mering, C. STRING V11: Protein-Protein Association Networks with Increased Coverage, Supporting Functional Discovery in Genome-Wide Experimental Datasets. *Nucleic Acids Res.* **2019**, *47*, D607−D613.

(20) Stanley, D.; Chambers, P. J.; Stanley, G. A.; Borneman, A.; Fraser, S. Transcriptional Changes Associated with Ethanol Tolerance in *Saccharomyces cerevisiae*. *Appl. Microbiol. Biotechnol.* **2010**, *88*, 231−239.

(21) Zanelli, C. F.; Maragno, A. L. C.; Gregio, A. P. B.; Komili, S.; Pandolfi, J. R.; Mestriner, C. A.; Lustri, W. R.; Valentini, S. R. EIF5A Binds to Translational Machinery Components and Affects Translation in Yeast. *Biochem. Biophys. Res. Commun.* **2006**, *348*, 1358−1366.

(22) Kang, H. A.; Hershey, J. W. Effect of Initiation Factor EIF-5A Depletion on Protein Synthesis and Proliferation of *Saccharomyces cerevisiae*. *J. Biol. Chem.* **1994**, *269*, 3934−3940.

(23) Zanelli, C. F.; Valentini, S. R. Pkc1 Acts through Zds1 and Gic1 to Suppress Growth and Cell Polarity Defects of a Yeast EIF5A Mutant. *Genetics* **2005**, *171*, 1571−1581.

(24) Auesukaree, C. Molecular Mechanisms of the Yeast Adaptive Response and Tolerance to Stresses Encountered during Ethanol Fermentation. *J. Biosci. Bioeng.* **2017**, *124*, 133−142.

(25) Chandler, M.; Stanley, G. A.; Rogers, P.; Chambers, P. A Genomic Approach to Defining the Ethanol Stress Response in the Yeast *Saccharomyces cerevisiae*. *Ann. Microbiol.* **2004**, *54*, 427−454.

(26) Yang, K.-M.; Lee, N.-R.; Woo, J.-M.; Choi, W.; Zimmermann, M.; Blank, L. M.; Park, J.-B. Ethanol Reduces Mitochondrial Membrane Integrity and Thereby Impacts Carbon Metabolism of *Saccharomyces cerevisiae*. *FEMS Yeast Res.* **2012**, *12*, 675−684.

(27) Stanley, D.; Fraser, S.; Stanley, G. A.; Chambers, P. J. Retrotransposon Expression in Ethanol-Stressed *Saccharomyces cerevisiae*. *Appl. Microbiol. Biotechnol.* **2010**, *87*, 1447−1454.

(28) Zakrzewska, A.; van Eikenhorst, G.; Burggraaff, J. E. C.; Vis, D. J.; Hoefsloot, H.; Delneri, D.; Oliver, S. G.; Brul, S.; Smits, G. J. Genome-Wide Analysis of Yeast Stress Survival and Tolerance

(29) Lebreton, A.; Saveanu, C.; Decourty, L.; Rain, J.-C.; Jacquier, A.; Fromont-Racine, M. A Functional Network Involved in the Recycling of Nucleocytoplasmic Pre-60S Factors. *J. Cell Biol.* **2006**, *173*, 349−360.

(30) de la Cruz, J.; Lacombe, T.; Deloche, O.; Linder, P.; Kressler, D. The Putative RNA Helicase Dbp6p Functionally Interacts With Rpl3p, Nop8p and the Novel Trans-Acting Factor Rsa3p During Biogenesis of 60S Ribosomal Subunits in *Saccharomyces cerevisiae*. *Genetics* **2004**, *166*, 1687−1699.

(31) Peng, W.-T.; Robinson, M. D.; Mnaimneh, S.; Krogan, N. J.; Cagney, G.; Morris, Q.; Davierwala, A. P.; Grigull, J.; Yang, X.; Zhang, W.; Mitsakakis, N.; Ryan, O. W.; Datta, N.; Jojic, V.; Pal, C.; Canadien, V.; Richards, D.; Beattie, B.; Wu, L. F.; Altschuler, S. J.; Roweis, S.; Frey, B. J.; Emili, A.; Greenblatt, J. F.; Hughes, T. R. A Panoramic View of Yeast Noncoding RNA Processing. *Cell* **2003**, *113*, 919−933.

(32) Zhang, L.; Wu, C.; Cai, G.; Chen, S.; Ye, K. Stepwise and Dynamic Assembly of the Earliest Precursors of Small Ribosomal Subunits in Yeast. *Genes Dev.* **2016**, *30*, 718−732.

(33) Chaker-Margot, M.; Hunziker, M.; Barandun, J.; Dill, B. D.; Klinge, S. Stage-Specific Assembly Events of the 6-MDa Small-Subunit Processome Initiate Eukaryotic Ribosome Biogenesis. *Nat. Struct. Mol. Biol.* **2015**, *22*, 920−923.

(34) Koch, B.; Mitterer, V.; Niederhauser, J.; Stanborough, T.; Murat, G.; Rechberger, G.; Bergler, H.; Kressler, D.; Pertschy, B. Yar1 Protects the Ribosomal Protein Rps3 from Aggregation. *J. Biol. Chem.* **2012**, *287*, 21806−21815.

(35) Cang, Y.; Prelich, G. Direct Stimulation of Transcription by Negative Cofactor 2 (NC2) through TATA-Binding Protein (TBP). *Proc. Natl. Acad. Sci. U.S.A.* **2002**, *99*, 12727−12732.

(36) Kim, S.; Cabane, K.; Hampsey, M.; Reinberg, D. Genetic Analysis of the YDR1-BUR6 Repressor Complex Reveals an Intricate Balance among Transcriptional Regulatory Proteins in Yeast. *Mol. Cell. Biol.* **2000**, *20*, 2455−2465.

(37) Beelman, C. A.; Parker, R. Degradation of MRNA in Eukaryotes. *Cell* **1995**, *81*, 179−183.

(38) Huang, Y.; Carmichael, G. G. Role of Polyadenylation in Nucleocytoplasmic Transport of MRNA. *Mol. Cell. Biol.* **1996**, *16*, 1534−1542.

(39) Sachs, A. B.; Sarnow, P.; Hentze, M. W. Starting at the Beginning, Middle, and End: Translation Initiation in Eukaryotes. *Cell* **1997**, *89*, 831−838.

(40) Helmling, S.; Zhelkovsky, A.; Moore, C. L. Fip1 Regulates the Activity of Poly(A) Polymerase through Multiple Interactions. *Mol. Cell. Biol.* **2001**, *21*, 2026−2037.

(41) Chang, Y.-F.; Carman, G. M. CTP Synthetase and Its Role in Phospholipid Synthesis in the Yeast *Saccharomyces cerevisiae*. *Prog. Lipid Res.* **2008**, *47*, 333−339.

(42) Mayer, M. L.; Gygi, S. P.; Aebersold, R.; Hieter, P. Identification of RFC(Ctf18p, Ctf8p, Dcc1p): An Alternative RFC Complex Required for Sister Chromatid Cohesion in *S. cerevisiae*. *Mol. Cell* **2001**, *7*, 959−970.

(43) Ma, M.; Liu, Z. L. Mechanisms of Ethanol Tolerance in *Saccharomyces cerevisiae*. *Appl. Microbiol. Biotechnol.* **2010**, *87*, 829−845.

(44) Ohta, E.; Nakayama, Y.; Mukai, Y.; Bamba, T.; Fukusaki, E. Metabolomic Approach for Improving Ethanol Stress Tolerance in *Saccharomyces cerevisiae*. *J. Biosci. Bioeng.* **2016**, *121*, 399−405.

(45) Scott, C. M.; Kruse, K. B.; Schmidt, B. Z.; Perlmutter, D. H.; McCracken, A. A.; Brodsky, J. L. ADD66, a Gene Involved in the Endoplasmic Reticulum-Associated Degradation of Alpha-1-Antitrypsin-Z in Yeast, Facilitates Proteasome Activity and Assembly. *Mol. Biol. Cell* **2007**, *18*, 3776−3787.

(46) Travers, K. J.; Patil, C. K.; Wodicka, L.; Lockhart, D. J.; Weissman, J. S.; Walter, P. Functional and Genomic Analyses Reveal an Essential Coordination between the Unfolded Protein Response and ER-Associated Degradation. *Cell* **2000**, *101*, 249−258.

(47) Halbleib, K.; Pesek, K.; Covino, R.; Hofbauer, H. F.; Wunnicke, D.; Hänelt, I.; Hummer, G.; Ernst, R. Activation of the Unfolded Protein Response by Lipid Bilayer Stress. *Mol. Cell* **2017**, *67*, 673−684.e8.

(48) Jing, H.; Liu, H.; Zhang, L.; Gao, J.; Song, H.; Tan, X. Ethanol Induces Autophagy Regulated by Mitochondrial ROS in *Saccharomyces cerevisiae*. *J. Microbiol. Biotechnol.* **2018**, *28*, 1982−1991.

(49) Horie, T.; Kawamata, T.; Matsunami, M.; Ohsumi, Y. Recycling of Iron via Autophagy Is Critical for the Transition from Glycolytic to Respiratory Growth. *J. Biol. Chem.* **2017**, *292*, 8533−8543.

(50) Rinnerthaler, M.; Jarolim, S.; Heeren, G.; Palle, E.; Perju, S.; Klinger, H.; Bogengruber, E.; Madeo, F.; Braun, R. J.; Breitenbach-Koller, L.; Breitenbach, M.; Laun, P. MMI1 (YKL056c, TMA19), the Yeast Orthologue of the Translationally Controlled Tumor Protein (TCTP) Has Apoptotic Functions and Interacts with Both Microtubules and Mitochondria. *Biochim. Biophys. Acta, Bioenerg.* **2006**, *1757*, 631−638.

(51) Biteau, B.; Labarre, J.; Toledano, M. B. ATP-Dependent Reduction of Cysteine−Sulphinic Acid by S. cerevisiae Sulphiredoxin. *Nature* **2003**, *425*, 980−984.

(52) Winder, S. J.; Jess, T.; Ayscough, K. R. SCP1 Encodes an Actin-Bundling Protein in Yeast. *Biochem. J.* **2003**, *375*, 287−295.

(53) Gourlay, C. W.; Carpp, L. N.; Timpson, P.; Winder, S. J.; Ayscough, K. R. A Role for the Actin Cytoskeleton in Cell Death and Aging in Yeast. *J. Cell Biol.* **2004**, *164*, 803−809.

(54) Nakatsukasa, K.; Nishimura, T.; Byrne, S. D.; Okamoto, M.; Takahashi-Nakaguchi, A.; Chibana, H.; Okumura, F.; Kamura, T. The Ubiquitin Ligase SCFUcc1 Acts as a Metabolic Switch for the Glyoxylate Cycle. *Mol. Cell* **2015**, *59*, 22−34.

(55) Kozjak, V.; Wiedemann, N.; Milenkovic, D.; Lohaus, C.; Meyer, H. E.; Guiard, B.; Meisinger, C.; Pfanner, N. An Essential Role of Sam50 in the Protein Sorting and Assembly Machinery of the Mitochondrial Outer Membrane. *J. Biol. Chem.* **2003**, *278*, 48520−48523.

(56) Green, R.; Lesage, G.; Sdicu, A.-M.; Ménard, P.; Bussey, H. A Synthetic Analysis of the *Saccharomyces cerevisiae* Stress Sensor Mid2p, and Identification of a Mid2p-Interacting Protein, Zeo1p, That Modulates the PKC1-MPK1 Cell Integrity Pathway. *Microbiology* **2003**, *149*, 2487−2499.

(57) Nguyen, H. P.; Du Le, H.; Man Le, V. V. Effect of Ethanol Stress on Fermentation Performance of *Saccharomyces cerevisiae* Cells Immobilized on Nypa Fruticans Leaf Sheath Pieces. *Food Technol. Biotechnol.* **2015**, *53*, 96−101.

(58) Ding, J.; Huang, X.; Zhang, L.; Zhao, N.; Yang, D.; Zhang, K. Tolerance and Stress Response to Ethanol in the Yeast *Saccharomyces cerevisiae*. *Appl. Microbiol. Biotechnol.* **2009**, *85*, 253−263.

(59) Kim, S.; Kim, J.; Song, J. H.; Jung, Y. H.; Choi, I.-S.; Choi, W.; Park, Y.-C.; Seo, J.-H.; Kim, K. H. Elucidation of Ethanol Tolerance Mechanisms in *Saccharomyces cerevisiae* by Global Metabolite Profiling. *Biotechnol. J.* **2016**, *11*, 1221−1229.

(60) Kennedy, E. J.; Pillus, L.; Ghosh, G. Pho5p and Newly Identified Nucleotide Pyrophosphatases/ Phosphodiesterases Regulate Extracellular Nucleotide Phosphate Metabolism in *Saccharomyces cerevisiae*. *Eukaryotic Cell* **2005**, *4*, 1892−1901.

(61) Strogolova, V.; Orlova, M.; Shevade, A.; Kuchin, S. Mitochondrial Porin Por1 and Its Homolog Por2 Contribute to the Positive Control of Snf1 Protein Kinase in *Saccharomyces cerevisiae*. *Eukaryotic Cell* **2012**, *11*, 1568−1572.

(62) Kim, J.-H.; Roy, A.; Jouandot, D.; Cho, K. H.; Cho, K. H. The Glucose Signaling Network in Yeast. *Biochim. Biophys. Acta, Gen. Subj.* **2013**, *1830*, 5204−5210.

(63) Miyata, N.; Fujii, S.; Kuge, O. Porin Proteins Have Critical Functions in Mitochondrial Phospholipid Metabolism in Yeast. *J. Biol. Chem.* **2018**, *293*, 17593−17605.

(64) de Sousa Abreu, R.; Penalva, L. O.; Marcotte, E. M.; Vogel, C. Global Signatures of Protein and MRNA Expression Levels. *Mol. Biosyst.* **2009**, *5*, 1512−1526.

(65) Hose, J.; Yong, C. M.; Sardi, M.; Wang, Z.; Newton, M. A.; Gasch, A. P. Dosage Compensation Can Buffer Copy-Number Variation in Wild Yeast. *eLife* **2015**, *4*, No. e05462.

(66) Romano, G. H.; Harari, Y.; Yehuda, T.; Podhorzer, A.; Rubinstein, L.; Shamir, R.; Gottlieb, A.; Silberberg, Y.; Pe'er, D.; Ruppin, E.; Sharan, R.; Kupiec, M. Environmental Stresses Disrupt Telomere Length Homeostasis. *PLoS Genet.* **2013**, *9*, No. e1003721.

(67) Wotton, D.; Shore, D. A Novel Rap1p-Interacting Factor, Rif2p, Cooperates with Rif1p to Regulate Telomere Length in *Saccharomyces cerevisiae*. *Genes Dev.* **1997**, *11*, 748−760.

(68) Kyrion, G.; Boakye, K. A.; Lustig, A. J. C-Terminal Truncation of RAP1 Results in the Deregulation of Telomere Size, Stability, and Function in *Saccharomyces cerevisiae*. *Mol. Cell. Biol.* **1992**, *12*, 5159−5173.

(69) Krauskopf, A.; Blackburn, E. H. Rap1 Protein Regulates Telomere Turnover in Yeast. *Proc. Natl. Acad. Sci. U.S.A.* **1998**, *95*, 12486−12491.

(70) Benoun, J. M.; Lalimar-Cortez, D.; Valencia, A.; Granda, A.; Moore, D. M.; Kelson, E. P.; Fischhaber, P. L. Rad7 E3 Ubiquitin Ligase Attenuates Polyubiquitylation of Rpn10 and Dsk2 Following DNA Damage in *Saccharomyces cerevisiae*. *Adv. Biol. Chem.* **2015**, *5*, No. 61944.

(71) Ishii, T.; Funakoshi, M.; Kobayashi, H.; Sekiguchi, T. Yeast Irc22 Is a Novel Dsk2-Interacting Protein That Is Involved in Salt Tolerance. *Cells* **2014**, *3*, 180−198.

(72) Díaz-Martínez, L. A.; Kang, Y.; Walters, K. J.; Clarke, D. J. Yeast UBL-UBA Proteins Have Partially Redundant Functions in Cell Cycle Control. *Cell Div.* **2006**, *1*, No. 28.

(73) Aguilera, F.; Peinado, R. A.; Millán, C.; Ortega, J. M.; Mauricio, J. C. Relationship between Ethanol Tolerance, H+-ATPase Activity and the Lipid Composition of the Plasma Membrane in Different Wine Yeast Strains. *Int. J. Food Microbiol.* **2006**, *110*, 34−42.

(74) Scharnewski, M.; Pongdontri, P.; Mora, G.; Hoppert, M.; Fulda, M. Mutants of *Saccharomyces cerevisiae* Deficient in Acyl-CoA Synthetases Secrete Fatty Acids Due to Interrupted Fatty Acid Recycling. *FEBS J.* **2008**, *275*, 2765−2778.

(75) Leber, C.; Polson, B.; Fernandez-Moya, R.; Da Silva, N. A. Overproduction and Secretion of Free Fatty Acids through Disrupted Neutral Lipid Recycle in *Saccharomyces cerevisiae*. *Metab. Eng.* **2015**, *28*, 54−62.

(76) Jansuriyakul, S.; Somboon, P.; Rodboon, N.; Kurylenko, O.; Sibirny, A.; Soontorngun, N. The Zinc Cluster Transcriptional Regulator Asg1 Transcriptionally Coordinates Oleate Utilization and Lipid Accumulation in *Saccharomyces cerevisiae*. *Appl. Microbiol. Biotechnol.* **2016**, *100*, 4549−4560.

(77) Hanlon, S. E.; Xu, Z.; Norris, D. N.; Vershon, A. K. Analysis of the Meiotic Role of the Mitochondrial Ribosomal Proteins Mrps17 and Mrpl37 in *Saccharomyces cerevisiae*. *Yeast* **2004**, *21*, 1241−1252.

(78) Muid, K. A.; Kimyon, Ö.; Reza, S. H.; Karakaya, H. C.; Koc, A. Characterization of Long Living Yeast Deletion Mutants That Lack Mitochondrial Metabolism Genes DSS1, PPA2 and AFG3. *Gene* **2019**, *706*, 172−180.

(79) Heinisch, J. J.; Rodicio, R. Protein Kinase C in Fungi—More than Just Cell Wall Integrity. *FEMS Microbiol. Rev.* **2018**, *42*, No. fux051.

(80) McCusker, D.; Denison, C.; Anderson, S.; Egelhofer, T. A.; Yates, J. R.; Gygi, S. P.; Kellogg, D. R. Cdk1 Coordinates Cell-Surface Growth with the Cell Cycle. *Nat. Cell Biol.* **2007**, *9*, 506−515.